Letter

Vol. 42, No. 20 / October 15 2017 / Optics Letters 4231

Optics Letters

Laser-written polarizing directional coupler with reduced interaction length

I. V. Dyakonov,* M. Yu. Saygin, I. V. Kondratyev, A. A. Kalinkin, S. S. Straupe, and S. P. Kulik

Faculty of Physics, M.V. Lomonosov Moscow State University, Leninskije Gory 1, Moscow 119991, Russia

**Corresponding author: iv.dyakonov@physics.msu.ru*

Received 16 August 2017; revised 21 September 2017; accepted 23 September 2017; posted 25 September 2017 (Doc. ID 304768); published 13 October 2017

Integrated optical waveguides, manufactured with femtosecond laser writing (FSLW) technology, enable precise control and manipulation of light in complicated photonic chips. However, due to the intrinsically low anisotropy of FSLW waveguides, polarizing integrated devices have had a relatively large footprint. In this Letter, we demonstrate an approach based on stress-induced anisotropy, allowing us to decrease the size of polarizing directional couplers down to 3.7 mm, almost an order of magnitude shorter than previously reported. The measured extinction ratios at the wavelength of 808 nm are 16 dB and 20 dB for the horizontal and vertical polarizations, respectively. We provide a possible theoretical model for the observed effects.

OCIS codes: (130.0130) Integrated optics; (220.0220) Optical design and fabrication; (230.0230) Optical devices; (270.0270) Quantum optics.

https://doi.org/10.1364/OL.42.004231

The constantly increasing complexity of modern optical experiments necessitates the transition to an integrated architecture meeting the stringent requirements of scalability and robustness, which cannot be fulfilled by bulk optics setups [1]. Integrated optical technology has found numerous successful applications in classical [2] and quantum optics [3] and optical communications [4]. Since the first pioneering works demonstrating FSLW waveguides [5] and directional couplers [6], this technology has proved to be especially suitable for rapid prototyping using facilities commonly available in an optical laboratory [7,8]. For this reason, the FSLW technique became popular in the quantum optics community, where it was successfully used to produce complex circuits required for experiments in quantum information processing [9,10] and computing [11].

An ability to realize polarization transformations is desirable in any integrated architecture. This is especially valuable for quantum applications, where control over polarization may pave the way for performing operations with polarization-encoded qubits and, for example, enable on-chip experiments with hyper-entangled states [12]. Some source of birefringence is required to enable control over polarization in FSLW waveguides. This birefringence may come from several sources: it may be determined by the anisotropic shape of the waveguides and the guided modes [13], it may arise from the specific nano-grating structures induced by laser machining [14], or it may be induced by the anisotropic mechanical stress of the material in the process of fabrication [15]. Typically, all sources are present, and birefringence of the waveguiding structure results from the interplay of these contributions.

Integrated devices for polarization control fabricated with the FSLW technology were reported by several groups. These include polarizing directional couplers (analogous to polarizing beam splitters in bulk optics) [16,17] and partially polarizing couplers [18], as well as birefringent retarders and waveplates [19,20]. Unfortunately, the achieved birefringence in FSLW waveguides is very low, so polarization-sensitive components have to be large, which significantly hinders their use in complex integrated circuits. Several attempts to enhance anisotropic behavior have been reported [20,21], but polarizing integrated devices still occupy sufficiently larger space on a chip than the circuits employed to manipulate the photon path degree of freedom. Moreover, increasing the intrinsic birefringence of the waveguide may not be the best solution, since that inevitably leads to undesirable polarization rotation in the connecting segments and straight waveguides. Ideally, one wants to localize the area of high birefringence to the active area of the device, while keeping the birefringence of the waveguides low.

In this Letter, we demonstrate polarizing directional couplers (PDCs) in fused silica with very strong dependence of the coupling coefficient on polarization. We exploit anisotropic mechanical stress induced by FSLW by reducing the distance between the coupled waveguides as much as possible. Importantly, the waveguides themselves have low birefringence outside the strongly coupled region.

The transmission properties of the PDCs are tuned by the proper choice of the interaction length L and the distance d between the adjacent waveguides inside the interaction region. In analogy with a bulk optical beam splitter, we define the effective transmission T and reflection R coefficients for an integrated PDC as the ratio of the power at the corresponding output ports to the total output power. Traditionally, the dependence of $T(R)$ on the interaction length is quantified by the coupling rate coefficients, which are generally different for two polarization states, C_H and C_V, due to anisotropy. Both differences in effective indices and mode profiles contribute to the polarization dispersion of a PDC:

$$C_{H,V} \sim \iint_{\mathbb{R}^2} \Delta n_{H,V}(x,y) u_{1H,V}(x,y) u_{2H,V}(x,y) \mathrm{d}x\mathrm{d}y, \quad (1)$$

where $\Delta n_{H,V}(x,y)$ is the refractive index contrast of the $H(V)$ polarized mode, and $u_{jH,V}(x,y)$ are the corresponding spatial mode functions. As a consequence, the beat lengths of the H and V modes differ, allowing the choice of an optimal interaction length of the PDC corresponding to the distribution of orthogonally polarized states of light to distinct output modes of the coupler. FSLW directional couplers are typically designed with weak coupling, thus enlarging the beat length, and they also exhibit rather low induced anisotropy, on the order of $\Delta n_{\mathrm{anis}} \sim 10^{-6}$ [20,22]. Recent works have demonstrated the potential of fused silica for an order of magnitude higher anisotropic structures fabrication [20,21]. Their approach is based on stress-induced anisotropy emerging in waveguiding structures in the presence of a non-guiding defect close to the waveguide core. We instead intend to demonstrate strong anisotropic coupling in a system of two closely spaced optical waveguides. We seek the optimal geometry of a PDC to shorten the interaction length required to spatially separate the orthogonal polarization states. The interaction length corresponding to a perfect splitting of orthogonal polarization states is $L_{\mathrm{pdc}} = \pi/(2|C_V - C_H|)$, which gives an exact value of L_{pdc}. In order to minimize the footprint of the PDC structure, the interacting optical modes have to be brought as close as possible, thus increasing the absolute values of C_H and C_V to resolve anisotropic behavior on a smaller scale. Moreover, shrinking the distance between the waveguides at some point brings up stress-induced anisotropic effects described in Refs. [20,21]. The mechanical stress field present in the material after the inscription of the first waveguide of a directional coupler affects the writing conditions for a second waveguide, resulting in increased anisotropy and propagating constants mismatch between the modes guided in two adjacent structures. However, as we will see below, this stress may also cause detrimental effects for PDCs, causing incomplete coupling and reducing extinction ratio.

For our purposes, we exploited 50 × 50 × 5 mm fused silica slabs (JGS1 glass, AG Optics). The sample is exposed to tightly (0.7 NA) focused 400 fs pulses from the frequency doubled ytterbium fiber laser (515 nm) with ≈80 nJ pulse energy delivered at 3 MHz repetition rate. To achieve uniform modification, the polarization of the impinging writing beam is oriented parallel to the waveguide writing direction, and the sample is translated along the focal spot at a moderate feed rate of 0.5 mm/s. We used a single-scan technique with no beam shaping. The details of our fabrication setup may be found in Ref. [23]. The birefringence axis of the waveguide is oriented perpendicular to the sample surface. The waveguides are designed to be single mode for wavelengths around 810 nm. The waveguide cross-section and mode field profiles for the two orthogonal polarizations are shown in Fig. 1. From the mode profiles, we estimate the refractive index contrast to be 4×10^{-3}. The propagation loss for the waveguides is 2 dB/cm, and it is polarization-independent.

We fabricated 5 arrays of PDCs of standard design with synchronously bending waveguides in the in-coupling and out-coupling regions and a straight interaction segment, as shown in Fig. 1(a). The distance between the waveguides in the interaction region d is identical within the array, and the interaction length L varies. The polarization properties of the fabricated PDC structures were studied with the simple transmission measurement setup. Linearly polarized (H or V) laser light at 808 nm was sent to one of the input ports of the directional coupler. The light from the output ports of the structures was collimated and sent to the power meter, positioned ≈1.5 m apart from the collimating lens, thus ensuring that the measured light power corresponds only to the guided mode. The results are presented in Fig. 2. We observe weak polarization sensitivity in the PDC structures with $d = 6$ μm and $d = 7$ μm.

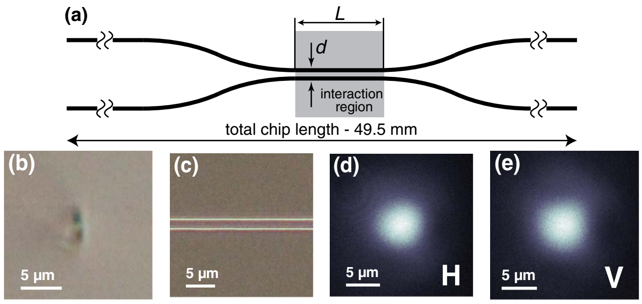

Fig. 1. Schematic of the integrated PDC (a). DIC microscope images of the fabricated waveguide cross-section (b) and interaction region of the $d = 3$ μm directional coupler (c). Images of the horizontal (d) and vertical (e) waveguide eigenmode profiles, respectively. Mode field diameters, obtained from these profiles are (4.76 ± 0.02) μm for the horizontally and (4.72 ± 0.02) μm for the vertically polarized modes. Analysis of the mode profiles yielded that the fabricated waveguides exhibit almost vanishing intrinsic birefringence on the order of 10^{-6}.

For almost symmetric waveguides, the only way to introduce stronger anisotropy is to reduce the distance between the waveguides. However, placing the waveguides close to each over comes at a price: as may be clearly seen from Figs. 2(a) and 2(b), the birefringence indeed increases for closer waveguides, but the oscillations of power between the waveguides are damped. This effect is becoming more pronounced for couplers with a smaller distance between the waveguides, as evidenced by Fig. 2(a). We attribute this phenomenon to the manifestation of the irregularities appearing in the process of writing a waveguide in close proximity to another one.

Let us introduce a theoretical model that explains the observed behavior. In the following, we will consider a single polarization mode and omit the polarization indices. Evolution of the field amplitudes $a_1(z)$ and $a_2(z)$ in the two arms of the interaction region of the coupler may be described by the coupled modes equations [24]:

$$\begin{cases} \frac{da_1}{dz} = -i\beta_1(z)a_1 - iCa_2, \\ \frac{da_2}{dz} = -iCa_1 - i\beta_2(z)a_2, \end{cases} \quad (2)$$

where $\beta_j(z)$ is the wavenumber dependent on the propagation coordinate due to the irregular modification of the mode's effective refractive indices ($j = 1, 2$). Equation (2) do not take loss in the waveguides into account, since it is trivial to do so under the plausible assumption of equal loss. Thus, one can show that the total optical power is conserved: $|a_1(z)|^2 + |a_2(z)|^2 = |a_1(0)|^2 + |a_2(0)|^2$, and the evolution described by (2) is unitary.

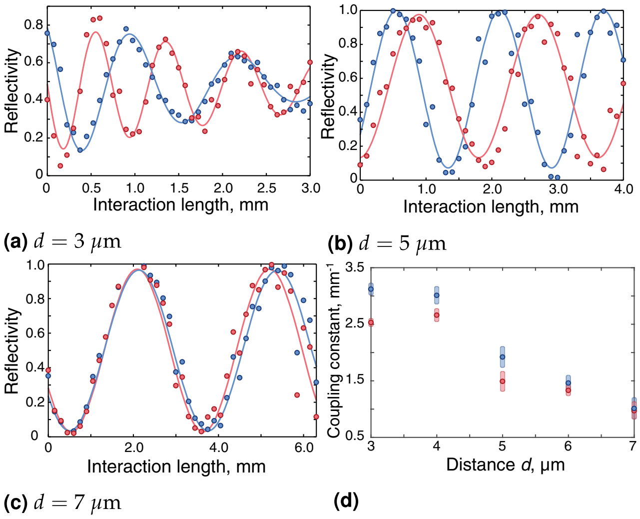

Fig. 2. Measured reflection coefficients for the arrays of the directional couplers fabricated with different distance d in the interaction region. (a)–(c) Anisotropic coupling inside the interaction region (horizontal polarization—red, vertical—blue). Strong anisotropy is clearly seen at (a) and (b), corresponding to closely spaced waveguides, whereas (c) shows weak anisotropic coupling due to the lack of stress-induced effects. Dependence of the coupling coefficients $C_{H,V}$ on the distance between the waveguides inferred from the theoretical fit is shown in (d), and shaded regions correspond to standard errors for mean predictions obtained from the fit.

One can split the wavenumber into two parts: $\beta_j(z) = \beta_{j0} + \delta\beta_j(z)$, with β_{j0} being the constant part and $\delta\beta_j(z)$—the variable part, which is fluctuating irregularly. The precise form of the irregular part is unknown, but we assume that the characteristic length l_0 over which $\delta\beta_j(z)$ changes significantly is much smaller than the period of the amplitude oscillations induced by the evanescent coupling $L_0 = \pi/2C$. Under this assumption, Eq. (2) can be regarded as stochastic, with $\delta\beta_j(z)$ playing the role of random fluctuations. Since $l_0 \ll L_0$, the fluctuation properties are defined by the correlation functions: $\langle\delta\beta_j(z)\rangle = 0$, $\langle\delta\beta_j(z)\delta\beta_k(z')\rangle = 2D_{jk}\delta(z - z')$, where $\delta(x)$ is the Dirac delta function and parameters D_{jk} quantify the fluctuations intensity.

We take the coupling coefficient C to be constant, while accounting for possible variations in wavenumbers, which requires some justification. Indeed, the coefficient is calculated using Eq. (1), where both the refractive index contrast and the eigenmode profiles are influenced by fluctuations of the refractive index. Therefore, small variations of the refractive index contrast $\delta(\Delta n) \ll \Delta n$ imply small deviations in the coupling coefficient $\delta C \ll C$. Similarly, the same variations $\delta(\Delta n)$ yield a change in the wavenumber $\delta\beta_j = k\delta n_{\text{eff}} \ll \beta_j = kn_{\text{eff}}$, which, however, may be comparable to the values of C due to the typically large values of β_j, and thus may significantly influence the dynamics.

To calculate the statistical averages $p_j(z) = \langle|a_j(z)|^2\rangle$, it is convenient to first derive the equations for the quadratic quantities—the power difference $\Delta(z) = |a_1(z)|^2 - |a_2(z)|^2$ and the complex-valued product $\sigma(z) = a_1(z)a_2^*(z)$, which can be done straightforwardly using Eq. (2). Statistical averaging may be performed analytically under the assumption of noise Gaussianity: $\langle\exp(i\Phi(z)\rangle = \exp(-\frac{1}{2}\langle\Phi^2(z)\rangle)$. We arrive to the following set of equations for three real-valued functions $\Delta(z)$, $\sigma' = \operatorname{Re}\sigma$, and $\sigma'' = \operatorname{Im}\sigma$:

$$\begin{cases} \frac{d\langle\sigma\rangle}{dz} = iCe^{-Dz}e^{-i\beta z}\langle\Delta\rangle, \\ \frac{d\langle\Delta\rangle}{dz} = -4Ce^{-Dz}(\langle\sigma'\rangle\sin(\beta z) + \langle\sigma''\rangle\cos(\beta z)), \end{cases} \tag{3}$$

where $\beta = \beta_{20} - \beta_{10}$ and $D = D_{11} + D_{22} - 2D_{12}$. Let us note, D is the only parameter describing the fluctuations that enters the equations and may be obtained from the fit of the experimental data. Finally, one can obtain a single equation for the power difference from Eq. (3):

$$\frac{d^3\Delta}{dz^3} + 2D\frac{d^2\Delta}{dz^2} + (4C(z)^2 + D^2 + \beta^2)\frac{d\Delta}{dz} - 4C(z)^2 D\Delta = 0, \tag{4}$$

where $C(z) = C\exp(-Dz)$ is the coupling coefficient, damped due to the propagation constant fluctuations. These equations should be solved with the following initial conditions: $\Delta(0) = p_{10} - p_{20} = (2\xi - 1)p_0$, $\Delta'(0) = -4C\sqrt{\xi(\xi - 1)}p_0\sin\Delta\varphi$, and $\Delta''(0) = -4Cp_0(\sqrt{\xi(1-\xi)}[D\sin\Delta\varphi + \beta\cos\Delta\varphi] + C(2\xi - 1))$. Here, $\xi = p_{10}/p_0$ is the fraction of total power at the input of the first waveguide, and $\Delta\varphi = \arg(a_{10}a_{20}^*)$ is the phase difference between the input amplitudes. These initial conditions should be chosen to consider the constant residual coupling in the curved in- and out-coupling regions of the coupler, since our model is only valid in the interaction region, where d is fixed.

We were unable to find an analytical solution for Eq. (4) in the general case. The influence of each of the parameters on the power dynamics in the waveguides is illustrated in Fig. 3(a). Non-zero detuning β with no fluctuations ($D = 0$) leads to an incomplete power transfer between the waveguides (black line). In the opposite case of $\beta = 0$ and $D \neq 0$ (blue line), random fluctuations prohibit the power transfer, causing the exponential decay of the effective coupling coefficient $C(z)$. When both coefficients are non-zero (orange line), the behavior of the power distribution resembles the one observed in the experiment. We used the numerical solution of Eq. (4) to fit the experimental data in Fig. 2. For the $d = 3$ μm directional coupler, the fit returns $D_H = 0.6\ \text{mm}^{-1}$, $D_V = 0.383\ \text{mm}^{-1}$, $\beta_H = 4.63\ \text{mm}^{-1}$, and $\beta_V = 6.56\ \text{mm}^{-1}$; for the $d = 5$ μm structures, $D_{H,V}$ vanishes and $\beta_H = 1.74\ \text{mm}^{-1}$ and $\beta_V = 1.07\ \text{mm}^{-1}$. Fitting results show that $d = 5$ μm structures do not exhibit coupling coefficient

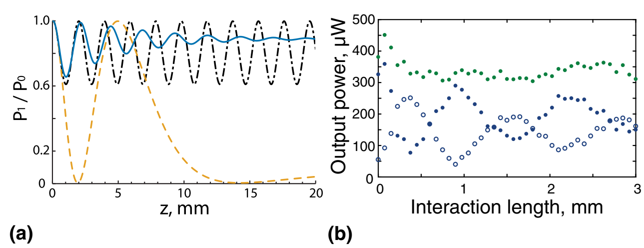

Fig. 3. (a) Dependence of the fraction of power in the first waveguide on the interaction length, obtained by numerically solving Eq. (4) (see text for details). (b) Measured power in both output arms of the directional coupler (blue dots and circles) and their sum (green dots) to illustrate the lack of additional loss in the interaction region. Input power was 3 mW, corresponding to 10 dB overall propagation loss for a 50 mm long structure.

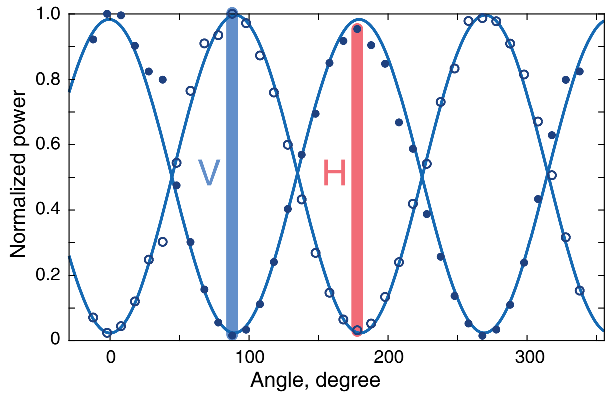

Fig. 4. Polarization extinction measurement for a completely polarizing integrated DC. Full circles represent the relative intensity in the reflected arm of the PDC, open circles are that in the transmitted arm. All data points are normalized to the maximal output intensity. Solid lines represent the Malus' law curve with R_H, R_V, or T_H, T_V as the fitting coefficients.

damping but preserve a highly anisotropic behavior. The observed behavior cannot be described by radiative losses in the coupled waveguides, since the total power in the interaction region is conserved, except the standard propagation loss, as shown in Fig. 3(b). No polarization-dependent loss was observed for the couplers, except for the case of $d = 3$ μm, where an additional 2 dB loss was measured for the horizontal mode.

The quality of the fabricated PDC ($d = 5$ μm, $L = 3.7$ mm) was established in the extinction measurement. We set the polarization state of the input laser beam by the Glan–Thompson polarizer and measured the intensity in each of the output ports of the structure. The dependencies obtained are shown in Fig. 4. The extinction ratios of the PDC may be inferred by fitting the obtained dependency with the Malus' law equation, accounting for non-ideal $R_{H,V}$, and $T_{H,V}$ and using values of 20 dB for the vertical and 16 dB for the horizontal input polarization state. Repeatable fabrication of high extinction integrated PDC devices is still a challenging task due to intrinsic random defects occurring during the writing process. That leads to fluctuations in the parameters of the couplers, clearly observed for longer interaction lengths in Fig. 2(b). However, to the best of our knowledge, the device reported in this work is the shortest polarizing directional coupler fabricated with femtosecond laser writing technology.

We have experimentally investigated anisotropically coupled FSLW waveguides in fused silica with spacing between the waveguides as small as 3 μm. Strong anisotropic coupling is observed for distances between the waveguides below 5 μm, leading to the reduced interaction length, which is required to realize a polarizing directional coupler. The demonstrated coupler has the measured extinction ratios of 16 dB and 20 dB for the horizontal and vertical polarizations, respectively, comparable to the state of the art FSLW integrated devices, but with an order of magnitude lower interaction length of 3.7 mm. The reduced footprint of the polarizing elements manufactured with our technique, together with low intrinsic birefringence of the interconnecting waveguides, makes our approach favorable for building complex polarization-sensitive integrated circuits.

Stronger anisotropic coupling for closely spaced waveguides is accompanied by some detrimental effects, manifesting themselves in the reduction of visibility of power oscillations for the coupled modes. We have observed the effect experimentally and provided a model, explaining the basic features of the observed behavior. Although the model qualitatively reproduces the observed effects, the underlying assumptions have to be tested in independent experiments, which we leave for future work. The observed effects of suppression of the power transfer for longer directional couplers with small spacing may be used to design couplers with unusual properties, such as the spectral dependence of the splitting ratio, and these opportunities will be investigated elsewhere.

Funding. Russian Science Foundation (RSF) (16-12-00017).

REFERENCES

1. A. P. Lund, M. J. Bremner, and T. C. Ralph, npj Quantum Inf. **3**, 15 (2017).
2. G. Koblmüller, B. Mayer, T. Stettner, G. Abstreiter, and J. J. Finley, Semicond. Sci. Technol. **32**, 053001 (2017).
3. J. O'Brien, B. Patton, M. Sasaki, and J. Vuckovic, New J. Phys. **15**, 035016 (2013).
4. C. R. Doerr, Front. Phys. **3**, 1 (2015).
5. K. M. Davis, K. Miura, N. Sugimoto, and K. Hirao, Opt. Lett. **21**, 1729 (1996).
6. K. Minoshima, A. M. Kowalevicz, E. P. Ippen, and J. G. Fujimoto, Opt. Express **10**, 645 (2002).
7. S. M. Eaton, W. Chen, L. Zhang, H. Zhang, R. Iyer, J. S. Aitchison, and P. R. Herman, IEEE Photon. Technol. Lett. **18**, 2174 (2006).
8. G. Della Valle, R. Osellame, and P. Laporta, J. Opt. A **11**, 013001 (2008).
9. G. D. Marshall, A. Politi, J. C. Matthews, P. Dekker, M. Ams, M. J. Withford, and J. L. O'Brien, Opt. Express **17**, 12546 (2009).
10. T. Meany, M. Gräfe, R. Heilmann, A. Perez-Leija, S. Gross, M. J. Steel, M. J. Withford, and A. Szameit, Laser Photon. Rev. **9**, 363 (2015).
11. A. Crespi, R. Osellame, R. Ramponi, D. J. Brod, E. F. Galvao, N. Spagnolo, C. Vitelli, E. Maiorino, P. Mataloni, and F. Sciarrino, Nat. Photonics **7**, 545 (2013).
12. M. A. Ciampini, A. Orieux, S. Paesani, F. Sciarrino, G. Corrielli, A. Crespi, R. Ramponi, R. Osellame, and P. Mataloni, Light Sci. Appl. **5**, e16064 (2016).
13. F. Kapron, N. Borrelli, and D. Keck, IEEE J. Quantum Electron. **8**, 222 (1972).
14. E. Bricchi, B. G. Klappauf, and P. G. Kazansky, Opt. Lett. **29**, 119 (2004).
15. B. McMillen and Y. Bellouard, Opt. Express **23**, 86 (2015).
16. L. A. Fernandes, J. R. Grenier, P. R. Herman, J. S. Aitchison, and P. V. Marques, Opt. Express **19**, 11992 (2011).
17. I. Pitsios, F. Samara, G. Corrielli, A. Crespi, and R. Osellame, "Geometrically-controlled polarisation processing in an integrated photonic platform," arXiv:1705.07739 (2017).
18. A. Crespi, R. Ramponi, R. Osellame, L. Sansoni, I. Bongioanni, F. Sciarrino, G. Vallone, and P. Mataloni, Nat. Commun. **2**, 566 (2011).
19. L. A. Fernandes, J. R. Grenier, P. R. Herman, J. S. Aitchison, and P. V. Marques, Opt. Express **19**, 18294 (2011).
20. R. Heilmann, M. Gräfe, S. Nolte, and A. Szameit, Sci. Rep. **4**, 4118 (2014).
21. L. A. Fernandes, J. R. Grenier, P. R. Herman, J. S. Aitchison, and P. V. Marques, Opt. Express **20**, 24103 (2012).
22. L. Sansoni, F. Sciarrino, G. Vallone, P. Mataloni, A. Crespi, R. Ramponi, and R. Osellame, Phys. Rev. Lett. **105**, 200503 (2010).
23. I. V. Dyakonov, A. A. Kalinkin, M. Y. Saygin, A. G. Abroskin, I. V. Radchenko, S. S. Straupe, and S. P. Kulik, Appl. Phys. B **122**, 245 (2016).
24. A. Snyder and J. Love, *Optical Waveguide Theory* (Chapman & Hall, 1983).